Ground-state statistics of directed polymers with heavy-tailed disorder

Thomas Gueudre and Pierre Le Doussal
CNRS–Laboratoire de Physique Théorique de l'Ecole Normale Supérieure, 24 Rue Lhomond, 75231 Cedex 05, Paris, France

Jean-Philippe Bouchaud
CFM, 21 Rue de l'Université, 75007 Paris, France

Alberto Rosso
Paris-Sud, LPTMS, UMR 8626, Orsay F-91405, France
(Received 6 November 2014; published 8 June 2015)

In this mostly numerical study, we reconsider the statistical properties of the ground state of a directed polymer in a $d = 1 + 1$ "hilly" disorder landscape, i.e., when the quenched disorder has power-law tails. When disorder is Gaussian, the polymer minimizes its total energy through a collective optimization, where the energy of each visited site only weakly contributes to the total. Conversely, a hilly landscape forces the polymer to distort and explore a larger portion of space to reach some particularly deep energy sites. As soon as the fifth moment of the disorder diverges, this mechanism radically changes the standard Kardar-Parisi-Zhang scaling behavior of the directed polymer, and new exponents prevail. After confirming again that the Flory argument accurately predicts these exponents in the tail-dominated phase, we investigate several other statistical features of the ground state that shed light on this unusual transition and on the accuracy of the Flory argument. We underline the theoretical challenge posed by this situation, which paradoxically becomes even more acute above the upper critical dimension.

DOI: 10.1103/PhysRevE.91.062110 PACS number(s): 05.40.−a, 68.35.Rh

I. INTRODUCTION

The so-called "directed polymer" (DP) problem has attracted an enormous amount of interest in the last 30 years [1–3]. It is a stylized model for the pinning of directed one-dimensional elastic objects (polymers, vortex lines, dislocations, etc.) by random impurities. It is perhaps the simplest model that captures the notion of "frustration" which is so crucial in many more complex disordered materials, such as spin glasses: the elasticity of the polymer competes with the energy of very favorable, but distant, pinning sites that would lead to a costly distortion of the polymer. The huge amount of work on this problem is justified not only because of its intrinsic interest, but also because it can be mapped to a host of other problems: the stochastic heat equation [4], itself mapped onto the Kardar-Parisi-Zhang (KPZ) equation [5] and the stochastic Burgers equation [6], population dynamics [7], problems of jammed transport [the totally asymmetric simple exclusion process (TASEP)], and crystal growth [8].

In $1 + 1$ dimensions (one transverse, one longitudinal, often taken as the "time" dimension), the problem is considered to be exactly solved, at least in some special limits and for some particular observables [9–16]. It is now well established that in the limit of "long" polymers of length $t \to \infty$, the transverse excursions x are of order t^{ζ} with $\zeta = 2/3$, i.e., much larger than $\sqrt{t}$, which would correspond to the thermal excursion of the polymer in the absence of disorder. Moreover, the total free-energy fluctuations scale with an anomalous exponent $\theta = 1/3$. More precisely, the total free energy of the polymer can be written as $-ct + \xi t^{1/3}$, where c is a nonuniversal constant and ξ is proportional to a random variable with a Tracy-Widom (TW) distribution, identical to the one governing the statistics of the largest eigenvalue of random matrices [the Gaussian orthogonal ensemble (GOE) or Gaussian unitary ensemble (GUE), depending on the boundary conditions] [12–16].

Although these scaling exponents have been known at the level of physical rigor since the 1980s [using replica theory [17], the exact stationary state of the corresponding KPZ equation [18], renormalization-group (RG) techniques [5], or mode-coupling theory [19]), it is fair to say that there is up to now apparently no simple, heuristic derivation of these exponents that would (a) unveil the deep physical origin of these results and (b) allow one to extend these results to other, similar problems, such as the directed polymer problem in $d + 1$ dimensions, for which the situation is still quite unclear [20–23] (although some progress has been made recently, notably in $2 + 1$ dimensions [21,24]). In particular, the existence of an upper critical dimension d_c beyond which $\zeta = 1/2$ even in the low-temperature, pinned phase, is still highly debated [25]. In $d = 1$ recent results have shown that the total free energy of the polymer can be written as $-ct + \xi t^{1/3}$, where c is a nonuniversal constant and ξ is proportional to a random variable with a Tracy-Widom distribution, identical to the one governing the statistics of the largest eigenvalue of random matrices (GOE or GUE, depending on the boundary conditions) [12–16].

In spite of numerous exact results, it is fair to say that even the $1 + 1$ directed polymer problem is far from understood. Consider, for example, the role of the distribution of the pinning energy in the large-scale properties of the polymer. One would naively expect that, as with many other problems, the existence and finiteness of the second moment of the distribution is enough to ensure that the above scaling results (valid for Gaussian or exponential disorder) hold asymptotically. Surprisingly, though, this does not seem to be the case. A heuristic, Flory-type argument that dates back

 ©2015 American Physical Society

from the early 1990s [26–28] suggests that as soon as the *fifth moment* of the distribution diverges, one should leave the realm of the standard DP or KPZ 2/3 scaling, and enter a new regime, where the extreme values taken by the pinning potential matter and change the scaling results. In fact, the same Flory argument suggests that the situation becomes worse and worse as the dimension increases—see [28] and Eq. (12) below. One expects any subexponential tail of the potential to play a crucial role at and above d_c. [In the different tree geometry, for example, it can indeed be checked explicitly that the Derrida-Spohn solution for DP on a tree indeed breaks down as soon as the potential has subexponential tails [29].]

The sensitive dependence of large-scale properties on the far tails of the disorder is certainly unusual and highlights our poor grasp of the standard (Gaussian) case. It also raises many technical questions; for example, about the validity of techniques that have been exploited in the context of Gaussian disorder, such as the replica method or the functional RG. It is clear that, if confirmed, these far-tail-induced effects would require new, specific theoretical methods that could, indirectly, shed added light on the DP problem altogether and perhaps beyond it. Before embarking on such a program, we wanted to reconsider the $1+1$ DP problem with heavy-tailed disorder, and establish numerically, as convincingly as possible, the violation of the standard DP or KPZ 2/3 scaling. Our results are, quite remarkably, in perfect agreement with the naive Flory predictions for the diffusion exponent ζ and the energy exponent θ, which confirms that the values $\zeta = 2/3$ and $\theta = 1/3$ and the whole Tracy-Widom statistics hold only if the probability density of the pinning energy V decays faster that $1/|V|^6$. We investigate several other statistical features of the ground state of the DP in the anomalous regime that shed light on this unusual transition and on the tenets of the Flory argument, namely, that the accessible extreme values of the pinning potential dominate the scaling behavior—a feature that we confirm directly; see, e.g., Figs. 3 and 11. One of the most interesting results of this study is our numerical determination of the generalization of the Tracy-Widom distribution for fat-tailed potentials, which appears to retain the standard $e^{-|s|^3}$ asymptotic TW behavior on one side of the distribution, but behaves as a power law (instead of $e^{-|s|^{3/2}}$) on the other side. We conclude with several open problems, underlying the theoretical challenge posed by this situation, which paradoxically becomes even more acute above the upper critical dimension.

II. THE MODEL

Here we consider a one-dimensional directed polymer growing on the two-dimensional square lattice depicted in Fig. 1. In what follows, we confine the study to the lowest-energy state of the polymer, as the temperature is expected to be irrelevant for the large-size limit.

Directed paths grow along the diagonals of the lattice with only (0,1) or (1,0) moves (hard-constraint condition), starting at (0,0) and with the second end left free. To each site of the lattice is associated an independent and identically distributed random number $V(x,t)$. The time coordinate is given by $t = i + j$ and the space coordinate by $x = (i - j)$. The total energy

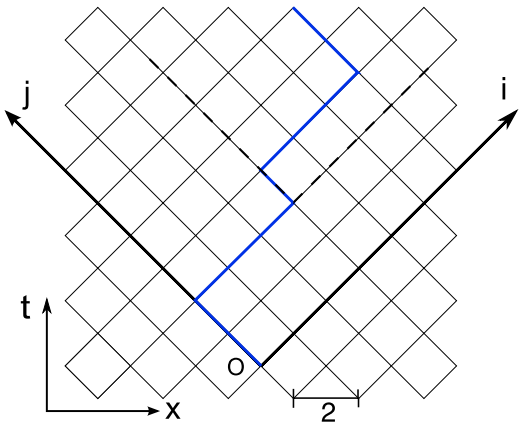

FIG. 1. (Color online) Sketch of the directed polymer model. The blue solid line corresponds to a polymer growing over the square lattice under the hard-constraint condition.

of the polymer is the minimum over all paths γ_t growing from (0,0) up to time t, defined as

$$E(t) = \min_{\gamma_t} \sum_{(x,\tau)\in\gamma_t} V(x,\tau) \tag{1}$$

with $x \in [\![-t,t]\!]$ and $\tau \in [\![0,t]\!]$. The energy of the polymer satisfies the following transfer matrix recurrence relation:

$$E_{x,t+1} = \min(E_{x-1,t}, E_{x+1,t}) + V(x,t+1) \tag{2}$$

with $E_{x,0} = \delta_{x,0}$. The free-end ground state is computed by taking the minimum of the energies over all end points $E(t) = \min_x E(x,t)$. In what follows, we use the shorthand notation $x(\tau)$ to describe the polymer path coordinate at time τ and $V(\tau) = V(x(\tau),\tau)$. In this paper, we study the properties of the DP for different disorder distributions $P(V)$; in particular we focus on the heavy-tailed probability distribution function (PDF) decaying as

$$P(V) \sim_{V\to-\infty} \frac{1}{|V|^{1+\mu}}. \tag{3}$$

It is known that, in one dimension, the search for an optimal path in a disorder landscape leads to excursions larger than the thermal ones, which are of order $\sqrt{t}$. The shape of the optimal path strongly depends on the underlying disorder landscape, as shown in Fig. 2. In particular, the excursions are more important for a heavy-tailed disorder than for a Gaussian disorder. Those differences correspond to different optimization strategies, as illustrated in Fig. 3:

(a) For a Gaussian disorder, the optimization strategy is *collective*: the total energy of the polymer is equally shared between all the sites.

(b) For a heavy-tailed PDF with $1 < \mu < 5$, the optimization strategy is *elitist*: an important fraction of the total energy is held by a small fraction of the sites belonging to the path.

(c) For a heavy-tailed PDF with $\mu < 1$, the optimization strategy is *individual*: most of the total energy of the polymer is localized on one particularly deep site.

Such differences in optimization have marked effects on the fluctuation properties at large t, in particular on the

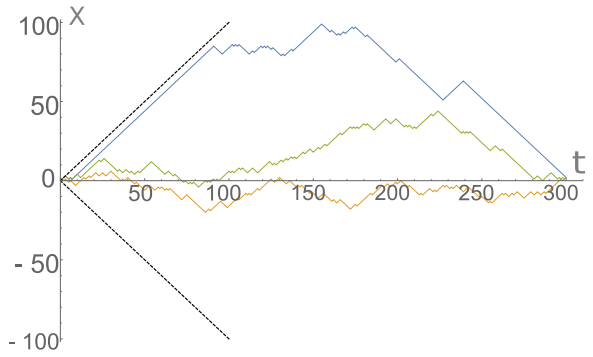

FIG. 2. (Color online) Optimal path ($t = 300$) for three different random environments: Gaussian disorder (lowest, in yellow), and heavy-tailed disorder with $\mu = 0.1$ (highest, in blue) and with $\mu = 2.5$ (middle, in green). The shape of the path is strongly affected by the underlying disorder. Because of the hard constraint, the path can evolve only inside the cone delimited by the dashed lines.

observables

$$\overline{x(t)^2} \sim t^{2\zeta}, \tag{4}$$

$$\overline{E(t)^2}^c = \overline{E^2(t)} - \overline{E(t)}^2 \sim t^{2\theta}. \tag{5}$$

Here θ and ζ are respectively the energy and the roughness exponents and show some universal features: they depend only on the behavior of the disorder tails, namely, the index μ. Note that other important quantities, such as the average energy $\overline{E(t)}$, strongly depend on all the microscopic details of the chosen model.

For a rapidly decaying disorder, the values of the exponents are known to be $\zeta = 2/3$ and $\theta = 1/3$ [17,18], which have been recently proved, via mathematical [9,30,31] and physical [10,15] approaches, for specific fast-decaying distributions such as the Gaussian, the exponential, or the log-gamma

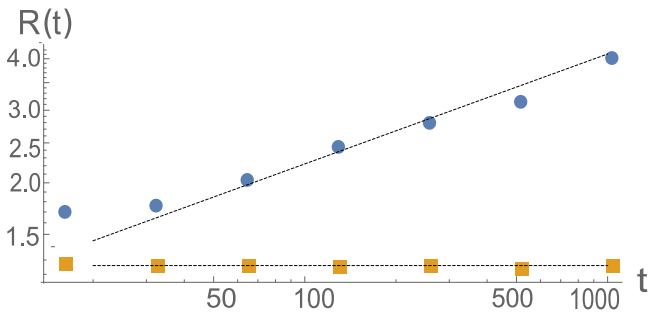

FIG. 3. (Color online) Ratio $R(t) = \min_{\tau<t} V(\tau)/\min_{\tau<t} X(\tau)$ of the minimum energy contribution along the ground state of a polymer of length t to the minimum of a sequence $\{X(\tau)\}$ of t random variables independently drawn from the very same disorder distribution, Eq. (3). Blue circles correspond to $\mu = 3$ and yellow squares to $\mu = 8$. The dashed lines plot either a constant (for $\mu = 8$) or $t^{\theta_\mu - 1/\mu} = t^{4/15}$ [using $\min_{\tau<t} X(\tau) \sim t^{1/\mu}$ and $\theta_3 = 3/5$]. One clearly sees that the optimal polymer for $\mu = 8$ performs hardly better than do purely random sequences; the elitist optimization for $\mu = 3$ leads to power-law growth of $R(t)$ with t, i.e., the optimization has led the polymer to go through much deeper sites.

distribution [32–35] (see also [17,18] for earlier, more heuristic arguments).

For heavy-tailed disorder, where extremes play a major role in the choice of the optimal path, the values of the exponents appear to rely on the balance between the energy of the deepest sites and the deformation energy it would cost to reach them [26–28]. This is formalized by the so-called Flory argument which we now recall briefly. Denoting by t the length and x the size of a typical excursion of the polymer, a result from the extreme statistics of heavy-tailed distributions gives, for the volume xt available to the polymer, an estimation of the energy of the deepest sites: $E_{\min} \sim -(xt)^{1/\mu}$. On the other hand, for the model with a hard constraint the deformation cost is entropic and, provided that $x \ll t$, follows a scaling similar to that of an elastic energy as $S \sim -x^2/t$. Balancing both estimations, $E_{\min} \sim S$, leads to the estimates

$$\zeta_\mu = \frac{1+\mu}{2\mu - 1}, \tag{6}$$

$$\theta_\mu = \frac{3}{2\mu - 1}. \tag{7}$$

We can guess that those formulas are valid for $2 < \mu < 5$, i.e., whenever $\zeta_\mu > 2/3$. Note that the values of the exponents are compatible with the scaling relation $\theta = 2\zeta - 1$. This relation comes from the statistical tilt symmetry (STS), originating in the invariance of the problem upon the tilting transformation $x(\tau) \to x(\tau) + \epsilon\tau$ in the large-scale limit [36].

Above $\mu = 5$, the Flory argument leads to $\zeta_\mu < 2/3$: instead of a strategy focusing on deep sites of the disorder, the behavior of the polymer is dominated by a collective strategy as in the Gaussian case. On the other hand, for $\mu = 2$ we have $\zeta_\mu = 1$ so that $x \sim t$ and the entropy cannot be approximated by an elastic energy. Due to the hard constraint, the excursions of the polymer are confined in a cone. This observation leads to another estimation of the exponents $\zeta_\mu = 1$ and $\theta_\mu = 2/\mu$ for $0 < \mu < 2$. Note that the STS symmetry is violated in that regime. All these Flory estimates are summarized in Table I.

When $\mu < 1$, the first moment of the disorder distribution diverges. That leads to a huge separation of energy scales in the disorder, where all the sites can be neglected compared to the value of the deepest site through which the optimal path has to go. Hence the optimization becomes *individual* and it allows the optimal path to be constructed recursively by picking the deepest site that pins the polymer and applying the same strategy among the sites inside the area delimited by the hard constraint. The term *greedy* was coined for such a hierarchical optimization strategy in Ref. [37], where some of its properties

TABLE I. θ_μ and ζ_μ as functions of μ. For $0 < \mu < 5$ the values of the exponents are estimated by scaling arguments. In contrast, in the collective optimization regime ($\mu > 5$) no simple scaling argument is known.

	$\mu > 5$	$5 > \mu > 2$	$2 > \mu > 0$
θ_μ	$1/3$	$3/(2\mu - 1)$	$2/\mu$
ζ_μ	$2/3$	$(1+\mu)/(2\mu - 1)$	1

were studied for the limit $\mu \to 0^+$. (Most notably, a complete characterization of the path geometry in this limit was obtained as a multifractal process, whose spectrum was computed.) Here we show that this approximation seemingly becomes asymptotically exact as $t \to \infty$ for all $\mu \leqslant 1$. In particular the end point distribution of the polymer is computed analytically for the greedy strategy and very well reproduces the numerical behavior for all $\mu < 1$.

III. NUMERICAL SIMULATIONS

In this section, we present numerical simulations done with the matrix transfer method, which allows us to keep track of both the energy and the position of the optimal path at every time t. The underlying disordered medium was generated using heavy-tailed distributions. Both a normalized Pareto and a Student t distribution of the tail index μ were used to ensure that the following results are not sensitive to the bulk of the distribution, but only to the tail, as expected.

We compare the numerical values of θ and ζ with the predictions of the (Flory) scaling arguments given in the the previous section, and obtain additional information about the whole PDF of the fluctuations of the total energy E. The Flory estimates have been conjectured (see [27]) to be a good approximation only in the limit $\mu \to 2^+$. However, a careful analysis of finite effects leads to the conclusion that the Flory argument may in fact be asymptotically exact [38]. Finally, we give strong numerical evidence of the existence of different optimization strategies as μ varies. This supports the correctness of the scaling argument in the regime of strong disorder for $\mu < 5$.

A. The scaling exponents

To measure the exponents θ and ζ, we can use the definitions given in Eq. (5). However, in Fig. 4, we observe that the statistical estimator for $\overline{E^2}^c$ never averages out when $\mu < 4$ and shows large jumps even for very large sampling sizes. Note that the statistical estimator of $\overline{E^2}^c$ converges only if both $\overline{E^2}^c$ and its statistical error $(\overline{E^4}^c/N)^{1/2}$ are finite. But, due to the presence of heavy tails in the disorder, high enough moments of the distribution of energy $P(E)$ could diverge. We will see in Sec. III B that for $2 < \mu < 4$, $\overline{E^2}^c$ is finite while $\overline{E^4}^c$ diverges.

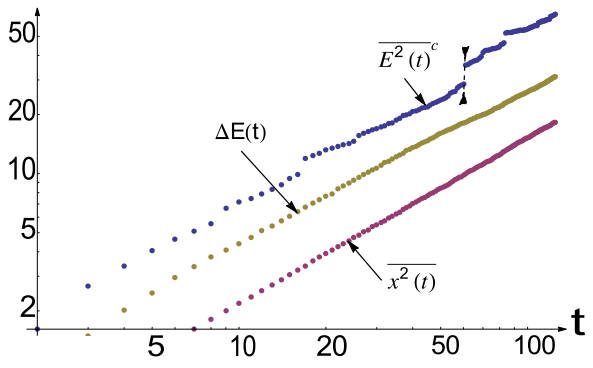

FIG. 4. (Color online) Stability analysis of our numerical results. The averages are performed over $N = 10^5$ samples. The mean squared displacement $\overline{x^2(t)}$ shows a well-defined smooth behavior, while the variance of the energy $\overline{E^2(t)}^c$ displays a jump around $t = 70$, which stems from a very deep single pin. This makes $\overline{E^2(t)}^c$ numerically unstable. On the contrary, for $\mu > 2$, the quantity $\Delta E(t)$ displays a well-defined behavior allowing for a reliable estimation of the exponent θ_{num}. Here $\mu = 3$ and $N = 2 \times 10^5$ samples.

TABLE II. Flory predictions of θ and ζ compared to numerical estimates for several values of μ. The agreement is extremely good (see also Figs. 5 and 6), except close to the transition value $\mu = 5$, where the numerical estimate is less precise due to important size effects.

μ	θ_μ	θ_{num}	ζ_μ	ζ_{num}
3	$3/5 = 0.60$	0.605 ± 0.006	$4/5 = 0.80$	0.802 ± 0.004
4	$3/7 \simeq 0.43$	0.44 ± 0.02	$5/7 \simeq 0.714$	0.715 ± 0.005
5	$1/3$	0.36 ± 0.03	$2/3$	0.69 ± 0.04
7	$1/3$	0.338 ± 0.008	$2/3$	0.669 ± 0.004

Another estimator of the spread of the distribution is the mean absolute deviation (MAD) ΔE:

$$\Delta E = \frac{1}{N} \sum_i |E_i - \overline{E}|. \tag{8}$$

This estimator is more resilient to extreme events and works better with heavy-tailed distributions. In contrast to the standard deviation, which squares the distance from the average, the MAD is well controlled as soon as the second moment of the PDF exists (in our case for $\mu > 2$), and allows us to properly extract θ_{num} (see Fig. 4). Note that $\overline{x^2(t)}$ does not present this kind of problem, because it is compactly supported due to the hard constraint (see Fig. 4).

The numerical values of the exponents for different values of μ, and their comparison with the Flory prediction, are summarized in Table II. The numerical estimations have been made with the maximum likelihood method. Figures 5 and 6 illustrate how good the Flory prediction is: see in

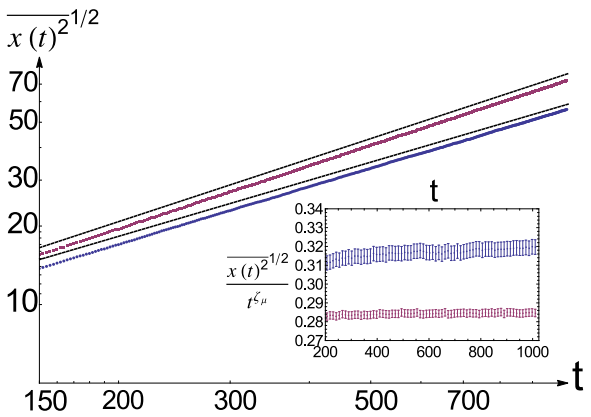

FIG. 5. (Color online) Mean square displacement of the end position of the optimal path for $\mu = 3$ (in red, above) and $\mu = 4$ (in blue, below). Dashed lines correspond to the Flory estimate given in Table I. Inset: $\overline{x(t)^2}/t^{\zeta_\mu}$ showing saturation at large t in both cases. $N = 2 \times 10^5$ samples.

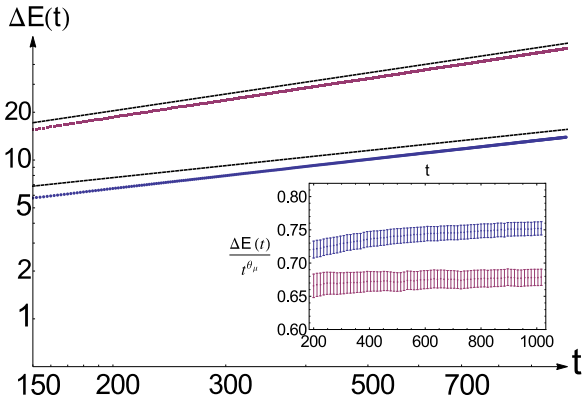

FIG. 6. (Color online) Mean absolute deviation ΔE of the optimal energy for $\mu = 3$ (in red, above) and $\mu = 4$ (in blue, below). Dashed lines correspond to the Flory estimate given in Table I. Inset: $\Delta E(t)/t^{\theta_\mu}$ showing saturation at large t in both cases. $N = 2 \times 10^5$ samples.

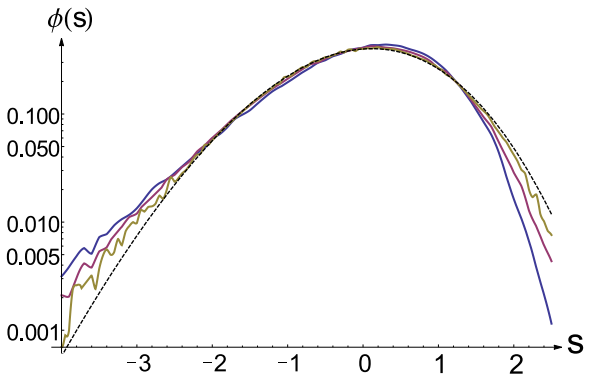

FIG. 7. (Color online) Collapse of the PDF $\phi(s)$, for several lengths (from the farthest from to the closest to the dashed line) $t = 2^4$ (blue), 2^7 (red), 2^8 (yellow) for a disorder PDF with $\mu = 8$. Comparison is made with the Tracy-Widom distribution F_2 after centering and rescaling (in dotted black). The average is over $N = 2 \times 10^5$ samples.

particular the insets where we show the quantities $\overline{x(t)^2}/t^{\zeta_\mu}$ and $\overline{|E - \overline{E}|}(t)/t^{\theta_\mu}$ which should saturate to a constant when $t \gg 1$ if the scaling argument is correct. The saturation time should, howeve, grow larger and larger as $\mu \to 5^-$, explaining the observed difference between results for $\mu = 3$ and $\mu = 4$. Indeed, in this limit, the strategy remains elitist, but the effect of deep sites is not as strong and needs a large value of t to be clearly distinguished from the rest of the "crowd." For $\mu > 5$, the strategy becomes collective, and the exponents $\theta = 1/3$ and $\zeta = 2/3$ are recovered.

B. Space and time fluctuations of the total energy

In this section, we present results for the probability distribution of the fluctuations of the ground-state energy E. The Gaussian (or fast-decaying disorder) case has been studied extensively in the past. On the other hand, there currently appears to be no study of its equivalent in heavy-tailed disorder.

It has been shown that, for some particular, fast-decaying disorder distributions (see [9,15,31]), after the proper rescaling, the probability distribution converges to a family of distributions, called the Tracy-Widom distributions. It is believed that this universality extends to all fast-decaying distributions. We define the rescaled variable

$$s(t) = [E(t) - \overline{E}(t)]/[\overline{E^2}^c(t)]^{1/2} \tag{9}$$

and show in Fig. 7 the rescaled energy distribution $\phi(s)$ for different μ's. (Note that, because we are interested in departure from the TW family, and for simplicity, we normalize the distribution to mean 0 and variance 1. For a finer characterization of the TW distribution, one could rely on more elaborate scalings as presented in Ref. [39]). It seems numerically clear that the TW universality class extends for any disorder with $\mu > 5$. Note that, for very negative s, $\phi(s)$ remains algebraic beyond some time dependent threshold $s < s_t^*$. However, when $t \to \infty$, the crossover towards the algebraic behavior s_t^* moves to $-\infty$.

On the contrary, for $0 < \mu < 5$, the limiting distribution is very different. The family of limiting distributions F_μ depends only on μ and on the boundary conditions. Its analytical expression is still unknown; inspired by results from extreme statistics, a natural guess would be the Frechet distribution $\mathbb{P}(X < x) = \exp(-a|x|^{-\mu'})$ or some convolutions thereof (see [28]). Similarly, one would intuitively assume that the tail exponents are preserved, as for the PDF of the minimum of independent random variables and so $\alpha = \mu$. However, the interplay with the elastic energy might lead to a shift in this exponent. This fact was already noticed in [40] for the model of a particle in a disorder landscape confined by a harmonic potential. In this simpler model, the shift can be understood heuristically as follows: Assuming again that the polymer is controlled by a very deep site, from record statistics, it is known that the tail of the distribution of the minimum of n heavy-tailed random variables decays as $\sim \frac{n}{|V|^{1+\mu}}$. Assuming that both elastic and potential energies scale similarly, this leads to the total energy of the polymer $E_{\rm tot} \sim u^2 \sim |V_{\rm min}|$ (where u denotes the typical lateral extension of the polymer) and therefore to $n \propto u \sim |V_{\rm min}|^{1/2}$. Hence the dependence of n on $V_{\rm min}$, inherent to the fact that large deviations in the disorder allow the particle to explore a larger space, which in turn leads to a modified exponent $\mu' = \mu - 1/2$ of the tail of the total energy. Since for the heavy-tailed directed polymer case, the ground state is supposedly controlled by a few deep sites, on which the elastic energy and potential compete in a similar way, the above argument could also possibly describe the tails, and yield $\mu' = \mu - 1/2$.

However, this exponent is rather hard to extract from numerics, as it comes from large deviations in the free-energy fluctuations, and hence from rare disorder realizations. Simulations up to $t = 2^{13}$ for more that $N = 2 \times 10^6$ samples nonetheless indicate a clear departure of μ' from the value μ and tend indeed to favor the above conjecture $\mu' = \mu - 1/2$ (see Fig. 8). Let us add that those numerical results indicate that the support of the limiting distributions F_μ is the whole real line, unlike the standard Frechet distribution for heavy-tailed extreme statistics. An interesting feature of F_μ is the fact that its right tail, corresponding this time to unfavorable configurations of the disorder, appears to decay as $e^{-\alpha s^3}$, similarly to the TW distribution. This fact would

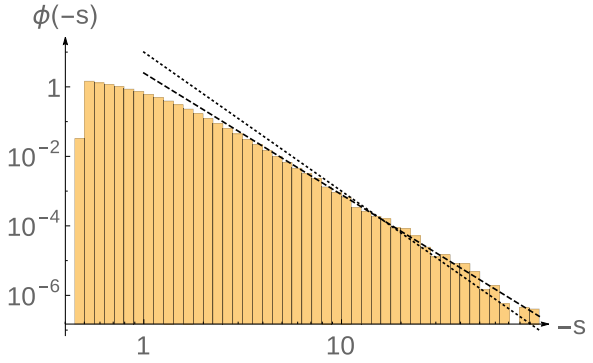

FIG. 8. (Color online) The algebraic left tail of $\phi(s)$ on a log-log scale, compared with decays of both exponents μ (dotted) and $\mu - 1/2$ (dashed), for $\mu = 3$. Polymers are of length $t = 2^{13}$, for a sampling of $N = 2 \times 10^6$ samples.

support a mixture of some Frechet and TW distributions as a possible guess and calls for further investigations of the typical properties of such large-deviation paths.

For future reference, the tail analysis of $F_\mu(s)$ for the special case $\mu = 3$ leads to the following numerical estimations: the left tail decays as $\int^s dx\, F_3(x) \approx 1.5\,|s|^{-2.5}$ for $s \to -\infty$ while for the right tail $F_3(s) \approx 1.8\, e^{-1.5 s^3}$ for $s \to \infty$ (see Fig. 9).

Let us now turn to the dependence of the ground-state energy on its final position $E(x,t)$, when the latter is imposed. In the Gaussian case, for infinite systems at large time, this process has been characterized as an Airy process, dependent on the initial conditions [41–44]. For small x, $E(x,t)$ behaves as a mere Brownian motion in x, but its correlations saturate for $x \gg t^{2/3}$ [45,46]. [It is worthwhile to mention that, in the discrete grid model used presently, $E(x,t)$ does not have Gaussian spatial increments, and these increments are in fact weakly correlated. Nonetheless, the correlation length does not grow with t and in the continuum limit $E(x,t)$ indeed converges (for small x) to a Brownian motion.] For a heavy-tailed disorder with $\mu > 5$, our results are consistent with the scenario where this convergence holds, as can be seen in the inset of Fig. 10.

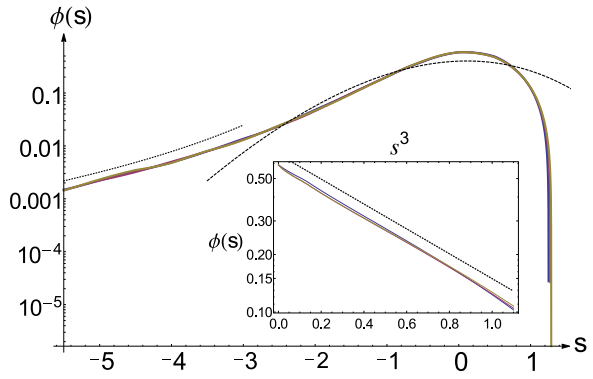

FIG. 9. (Color online) Collapse of $\phi(s)$, for several lengths $t = 2^4, 2^7, 2^{10}$ and for a disorder PDF with $\mu = 3$ (due to the weak finite-size effect, the various curves, drawn as solid lines, are indistinguishable). Comparison is made with the Tracy-Widom distribution F_2 after centering and rescaling (in dotted black). The decay estimate of index $\mu' = \mu - 1/2$ is plotted in dashed black. Inset: Far right tail of $\phi(s)$ compared to a decay of $e^{-1.5 s^3}$ (in dotted black). Average over $N = 2 \times 10^5$ samples.

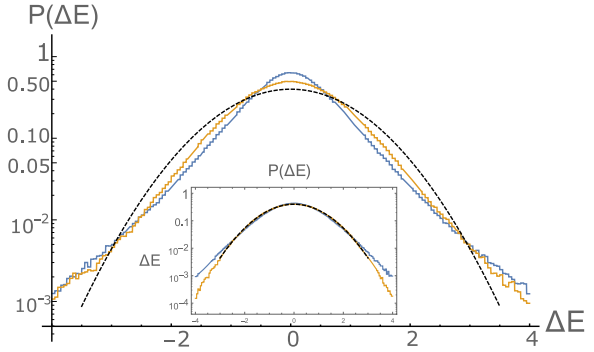

FIG. 10. (Color online) Probability distribution of ΔE for various sizes of the increments Δx of the stationary distribution for the disorder with $\mu = 3$: from the most peaked to the least, $\Delta x = 4$ (blue) and 64 (yellow). The variance of the distributions is normalized to 1. Tails survive even for large increments. The dashed black line is the Gaussian distribution. Inset: Same probability distributions for a disorder with $\mu = 8$, with convergence towards a Gaussian distribution at large increments. The time used in simulation is $t = 10^5$.

The situation is quite different in the elitist optimization strategy. Because the increments of the stationary process are controlled by the deep sites, they exhibit jumps of all sizes with power-law tails. Furthermore, the increments in energy $\Delta E(x)$ are, through scaling arguments, expected to behave as $\Delta E(x) \sim x^{\theta/\zeta}$ with $\theta/\zeta = 3/(1+\mu) > 1/2$ as soon as $\mu < 5$. Hence the time-stationary process of $E(x,t)$ is superdiffusive (in x), with strongly correlated heavy-tailed increments of index μ (see Fig. 10). A more precise characterization of this process (which is neither a fractional Brownian motion nor a Lévy walk) would be quite interesting and is left for future investigations. The analog of the Airy process for $\mu < 2$ was characterized in Refs. [37,47].

C. Zooming into the optimization strategies

Although the scaling argument gives the correct estimates, it relies on the assumption that the fluctuations of E are controlled by the fluctuations of the deepest sites in the disorder. This stems from the fact that the optimal path makes large excursions specifically to reach some favorable pinning sites. While for $\mu < 1$, one site dominates over all the the others, there is no such obvious dominance for $1 < \mu < 5$: there still exists a large population of sites with local energy of order $V_{\min}$. Hence to check the validity of the elitist optimization strategy, one has to test the fact that the optimal path indeed picks up *some* sites among the deepest available, whereas in the collective case this is not so.

We have therefore formulated the elitist optimization hypothesis as follows: Consider a paraboloid region $\mathcal{R}(\alpha)$ of length t and width $t^\alpha/2$, containing a number of sites proportional to $t^{1+\alpha}$. We then compute the probability $P_c(\alpha)$ that the minimum-energy site along the polymer is one among the $\mu \ln(t)$ deepest sites within the region $\mathcal{R}(\alpha)$. [The choice

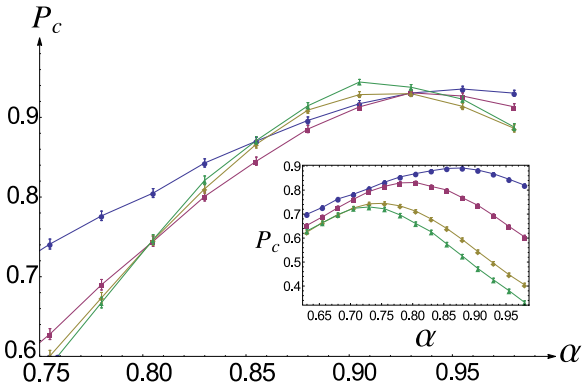

FIG. 11. (Color online) Probability $P_c(\alpha)$ as defined in the text for a heavy-tailed disorder with $\mu = 3$, corresponding to an elitist optimization. Symbols correspond to different lengths: $t = 2^6$ (circles), 2^9 (squares), 2^{11} (diamonds), 2^{12} (triangles). The averages are performed over $N = 2 \times 10^5$ samples. As expected, $P_c(\alpha)$ appears to peak around the value 0.9, which should converge to $\zeta_3 = 0.8$ for very large sizes. Inset: The same analysis performed for $\mu = 8$, corresponding to a collective optimization. In this case, $P_c(\alpha)$ decreases as a function of t, indicating that the minimum-energy site becomes less and less relevant as the size of the polymer increases.

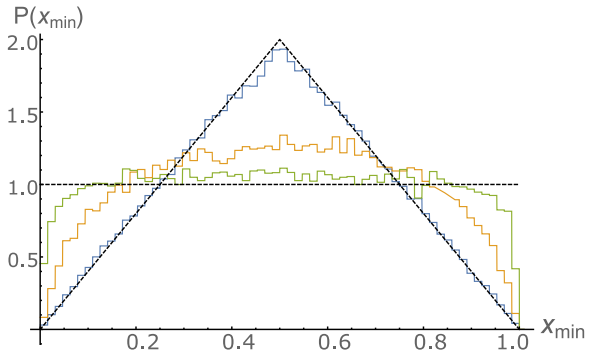

FIG. 12. (Color online) Histograms for $P(x_{min})$ of the position of the minimum x_{min} (normalized in [0,1]) of site energy *along* the polymer with both extremities fixed, for various disorder. From the most peaked to the flattest, $\mu = 0.5$ (blue) and 3 (yellow) and Gaussian disorder (green). In dashed black, both the uniform distribution and the distribution of the minimum for the greedy case, to which disorders with $\mu < 1$ converge. $t = 512$ and $N = 10^5$ samples. We expect that the distribution converges to a uniform distribution at large t for $\mu > 5$, but to remain nontrivial for $\mu < 5$.

of $\mu \ln t$ sites corresponds to a rough estimate of the number of completely independent paths in the region $\mathcal{R}(\alpha)$.]

Intuitively, we expect that for the elitist strategy, the minimum energy along the polymer should be deeper than the minimum restriced to $\mathcal{R}(\alpha) \subset \mathcal{R}(\zeta)$ when $\alpha < \zeta$. On the contrary, whenever $\alpha > \zeta$, the minimum along the polymer should be higher than the minimum in $\mathcal{R}(\alpha)$, since the elastic energy prevents it from reaching this particularly favorable site. Therefore, when $t \to \infty$, $P_c(\alpha)$ should become more and more peaked around $\alpha = \zeta$ for the elitist strategy. In the collective regime, on the other hand, $P_c(\alpha)$ should vanish for all α since the global optimization has nothingwhatsoever to do with the value of the deepest available site.

Figure 11 suggests a different qualitative behavior for $\mu = 3$ and $\mu = 8$, in agreement with the above prediction. Note that the maxima of the curves in Fig. 11 corresponding to an estimation of the rugosity exponent ζ are moving to the left as t increases. They are expected to converge towards $\zeta_3 = 4/5$ for $t \to \infty$, although the convergence appears to be very slow. Such a difference in optimization strategy is reflected in the extremal statistics observed *along* the polymer path. Granted the Gaussian optimal path is not relying on extremal sites, the position of the minimum-energy site should be (asymptotically) flat over $[1,t]$ (see Fig. 12), with finite-size effects coming from the smaller entropy at the very extremities of the polymer. On the other hand, for $\mu < 5$ and for periodic boundary conditions, the position of the minimum site is related to the maximum entropy of the polymer; hence the mode should be located right in the middle of the path. In the greedy case $\mu \to 0^+$, the probability distribution of this minimum is easily computed and represented in Fig. 12 as the limiting distribution for every disorder with $\mu < 1$.

IV. DISTRIBUTION OF THE END POINT

Another observable of interest is the distribution of the end point of the (unconstrained) optimal path. Compared to the fluctuations of the energy $E(t)$, we know much less about the statistics of $x(t)$. One expects the rescaled position $z = x(t)/t^\zeta$ to converge in fact towards a limiting distribution $Q_\zeta(z)$. In general, the analytic shape of $Q_\zeta(z)$ is unknown, although for the case $\zeta = 2/3$ and the particular case of an exponential distribution of the disorder [42] one can characterize the joint distribution of the position and total energy of the optimal path $\mathbb{P}(E(t),x(t))$. From this result, it has been shown that the marginal $Q_{2/3}(z)$ has an infinite support and is actually numerically very close to the Gaussian distribution, although it cannot be computed explicitly [48–50].

The heavy-tailed disorder case exhibits a radically different behavior, since $Q_\zeta(z)$ is strongly influenced by the large excursions of the optimal path to reach pinning sites. For $\mu < 2$, ζ saturates to 1 due to the hard constraint and the support of $Q_\mu(z)$ is reduced to the interval $[-1,1]$: the extremity has a finite probability to reach any point of the available space, even at large t.

Denoting $z = x(t)/t \in [-1,1]$, the distribution $Q_\mu(z)$ can be explicitly computed for the greedy strategy, where the optimization becomes a hierarchical recursive process. In the Appendix we give the details of the computation and our final result reads

$$Q_{\text{greedy}}(z) = \tfrac{3}{4}(1 - z^2). \tag{10}$$

This result *a priori* holds only in the limit $\mu \to 0$. However, it was argued in Sec. II that the greedy strategy should hold for every $\mu < 1$ at large times. This assumption is further confirmed by numerics for $Q_\mu(z)$ (see Fig. 13), retaining its parabolic shape until $\mu = 1$. For $\mu \in (1,2)$, the support still remains the interval $[-1,1]$, but $Q_\mu(z)$ is modified. The numerical results are relatively well fitted by the Beta distribution family $\mathbb{B}(\nu,\nu) = c_\nu(1 - x^2)^\nu$, where ν is a fitting parameter that depends on μ (see Fig. 13).

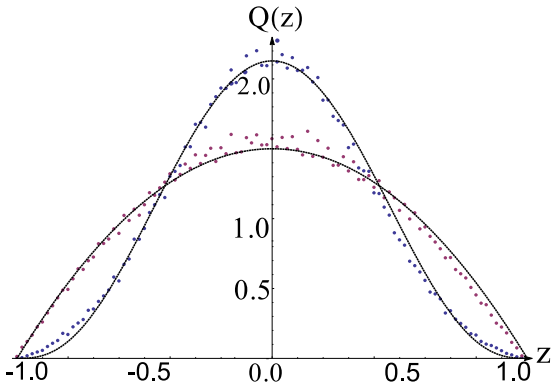

FIG. 13. (Color online) The PDF $Q(z)$ of the position of the free end as a function of $z = x(t)/t$. In blue (most peaked) for a disorder PDF of $\mu = 1.5$; in red (less peaked), $\mu = 0.5$. In dotted black, the theoretical parabolic prediction. We also show the symmetric Beta distribution fit, with $\nu = 3.8$. $t = 2^{11}$ and $N = 2 \times 10^5$.

Let us now consider the case $2 < \mu < 5$. We could expect that the tails of $Q_\mu(z)$ are again controlled by the position of the deepest available site. The decay exponents may therefore be inferred from the zero-dimensional particle model, as in Sec. III B above. This approach predicts [40]

$$Q_\mu(z) \sim \frac{1}{z^{2\mu}}. \tag{11}$$

In practice, it is delicate to estimate accurately the tail exponent of $Q_\mu(z)$, because of the presence of the cutoff imposed by the hard constraint of our discrete numerical model. Our results are nevertheless consistent with the above prediction Eq. (11). Such an algebraic tail is important conceptually when comparing with, e.g., the functional RG approach. Indeed, moments of the position are related to the moments of the renormalized disorder in that method [51]. In our case moments of sufficently high orders diverge, implying that the loop expansion of the standard Gaussian disorder case [52] needs to be reconsidered as soon as $\mu < 5$, even when the two-body correlator of the disorder is perfectly defined (i.e., when $\mu > 2$).

V. PERSPECTIVES

Finally, we mention briefly here how the present results extend to finite temperature and larger dimensions. The Flory argument can be easily extended to any dimension (as was done in Refs. [28,40]), predicting some fragility of the Gaussian regime with respect to the dimension d. The critical $\mu_c(d)$ is estimated as

$$\mu_c(d) = \frac{1 + d\zeta_G(d)}{2\zeta_G(d) - 1}. \tag{12}$$

Indeed, the larger the transverse space, the easier it is for the optimal path to visit deep sites, hence favoring the elitist strategy to the detriment of the collective one. As mentioned in the Introduction, the existence of an upper critical dimension d_c above which $\zeta_G = 1/2$ even in the low-temperature phase is still an open question. But from the Flory estimate above, we readily conclude that $\mu_c(d) = \infty$ for $d > d_c$, meaning that *any* heavy tail is expected to be relevant above d_c. This fragility is clearly apparent for the tree geometry, for which much of the model is solvable [29].

As for the case of finite temperatures, we expect that at least in low dimensions, the statistical properties studied in the present article should survive in the large-t limit, with the appearance of an additional thermal time scale below which the polymer behaves as a random walk. The possibility of an intermediate KPZ regime should also be investigated. The interplay between those various scales can be cast into a more quantitative framework, through simple Flory arguments or results from extremal statistics, and will be displayed elsewhere.

Finally, it should be noted that, albeit of very large interest, the access to finite-temperature and high-dimension regimes presents important difficulties even from a numerical point of view. As shown previously, the study of the asymptotic regime often requires rather long times. Coupled with the need for a large disorder space in high d, or the thermal average at finite T, it makes the simulations very difficult in practice.

VI. CONCLUSION

We presented a detailed investigation of the modification of the KPZ universality class due to heavy-tailed disorder, building upon several previous studies [26,27,37]. These modifications are deep: the KPZ universality class breaks down as soon as the fifth moment of the disorder diverges. From a standard renormalization procedure, one would have naively expected that the convergence of the second moment (the variance) of the disorder would suffice. As we emphasized in the Introduction, this paradox becomes even more acute above the upper critical dimension—see [28]. From a KPZ point of view, this shows that the interplay between nonlinearities and rare but large events is highly nontrivial and requires different analytical methods. Nonetheless, additional universality classes emerge, since both the exponents and corresponding probability distributions seem uniquely controlled by the behavior of the tail, the bulk of the disorder distribution being irrelevant.

However, our hope to get a better grasp on the KPZ class itself by studying the case of heavy-tailed potentials is clearly hindered by the lack of analytical tools. Exact results are scarce and numerical simulations have been extensively used to illuminate the situation. They indicate a sharp transition when the fifth moment of the distribution diverges, between the Gaussian KPZ or DP regime characterized by the standard exponents ($\theta = 1/3, \zeta = 2/3$) and some nontrivial values (θ_μ, ζ_μ) that seem to be exactly predicted by a simple Flory-like argument. The full ground-state energy distribution also changes from Tracy-Widom to a different family of functions, with a power-law tail for large negative values of the energy and the Tracy-Widom $e^{-|s|^3}$ behavior for anomalously "bad" ground-state energies. Several other quantites have been investigated—such as the process governing the energy as a function of the end point of the polymer or the distribution of this end point—which are also markedly different from their Gaussian counterparts in the tail-dominated regime. Finally, we have attempted to obtain direct evidence that the deepest available sites play a special role in the tail-dominated regime, giving support to the validity of the Flory argument. Still, there

are many outstanding open problems. For example, the largest eigenvalues of random matrices with heavy-tailed distributed entries are known to leave the Tracy-Widom universality class when the fourth moment (rather than the fifth) diverges [28]. This questions the existence of an exact mapping between the DP problem and random matrix ensembles for heavy-tailed disorder (see the discussion in Ref. [28]).

A very important issue (in our minds) is the extension of the functional RG approach to heavy-tailed situations. This might shed considerable light on the method itself and on the deep underlying mechanisms at play in pinning problems and in nonlinear (KPZ-like) stochastic partial differential equations. Our detailed numerical study of the directed polymer has unveiled that the appropriate statistics appears to possess an underlying recursive structure. This hypothesis is backed by the solvable "greedy" limit of an exponentially wide disorder. This calls for the development of theoretical tools able to handle these hierarchical processes.

ACKNOWLEDGMENT

P.L.D. acknowledges support from PSL Grant No. ANR-10-IDEX-0001-02-PSL.

APPENDIX: DERIVATION OF $Q_\mu(x)$ IN $\mu \to 0$

The derivation is eased by taking the continuum limit, where for convenience we rescale the position of the end point to $z \in [-1,1]$. We introduce the sequence of variables $\xi_i = \frac{x_i+y_i}{2}$ and $2r_i = y_i - x_i$, (x_i, y_i) which are the coordinates of the pinning site chosen at step i. The measure being uniform over the space of intervals, it stays uniform if we fix the center of mass, under the constraint that the end points cannot leave $[-1/2, 1/2]$. The joint probability distribution is, constrained on $[-1,1] \times [0,1]$,

$$P_0(\xi, r)d\xi\, dr = \Theta(r \leqslant 1 - |\xi|)d\xi\, dr. \tag{A1}$$

Due to self-similarity of the process, there are recursive relations between the end points after i steps and after $i+1$ steps. We are eventually interested in the limit of the following process z_∞, describing the position of the end point at $n \to \infty$:

$$z_\infty = \xi_1 + r_1\xi_2 + r_1 r_2 \xi_3 + \cdots . \tag{A2}$$

All pairs (ξ_i, r_i) have the same joint distribution P_0 and are independent for $i \neq j$. This bears some similarities with Kesten variables [53] but note that ξ_i and r_i are not independent themselves. The variable z_∞ obeys the following equation:

$$z_\infty =_{\text{law}} \xi + r z_\infty \tag{A3}$$

This leads to an integral equation for $P(z_\infty)$, the PDF of the end point; for example, if we choose to condition over the value of z_∞ in the above equation,

$$\begin{aligned} P(z) &= \int_{r,u} P_0(z - ru, r)P(u)du\, dr \\ &= \int_{r,u} \Theta(r < 1 - |z - ru|)P(u)du\, dr. \end{aligned} \tag{A4}$$

Although there is no generic way to solve such integral equations, we can recursively compute the moments or use the above equation to write down a differential equation for $\phi(\lambda) = E(e^{i\lambda z_\infty})$. Or one can simply check that a parabola $P(z) = \frac{3}{4}(1 - z^2)$ is the proper solution. $\Theta(r < 1 - |z - ru|)$ is non zero for $r < \frac{1+z}{1+x}$ if $z < x$ and $r < \frac{1-z}{1-x}$ if $x < z$. Hence, the right side of Eq. (A4) is equal to

$$\begin{aligned} &\frac{3}{4}\left(\int_{-1<x<z} \frac{1+z}{1+x}(1-x^2)dx + \int_{z<x<1} \frac{1-z}{1-x}(1-x^2)dx\right) \\ &\quad = \frac{3}{4}(1 - z^2). \end{aligned}$$

The result follows as given in Eq. (10).

[1] Timothy Halpin-Healy and Yi-Cheng Zhang, Kinetic roughening phenomena, stochastic growth, directed polymers and all that. Aspects of multidisciplinary statistical mechanics, Phys. Rep. **254**, 215 (1995).

[2] Paul Meakin, The growth of rough surfaces and interfaces, Phys. Rep. **235**, 189 (1993).

[3] Thomas Kriecherbauer and Joachim Krug, A pedestrian's view on interacting particle systems, KPZ universality and random matrices, J. Phys A **43**, 403001 (2010).

[4] Ivan Corwin, The Kardar-Parisi-Zhang equation and universality class, Random Matrices: Theory Appl. **01**, 1130001 (2012).

[5] Mehran Kardar, Giorgio Parisi, and Yi-Cheng Zhang, Dynamic scaling of growing interfaces, Phys. Rev. Lett. **56**, 889 (1986).

[6] Jérémie Bec and Konstantin Khanin, Burgers turbulence, Phys. Rep. **447**, 1 (2007).

[7] Thomas Gueudré, Alexander Dobrinevski, and Jean-Philippe Bouchaud, Explore or exploit? A generic model and an exactly solvable case, Phys. Rev. Lett. **112**, 050602 (2014).

[8] Joachim Krug and Herbert Spohn, Kinetic roughening of growing surfaces, in *C. Godreche* (Cambridge University Press, Cambridge 1991), Vol. 1, p. 1.

[9] Kurt Johansson, Shape fluctuations and random matrices, Commun. Math. Phys. **209**, 437 (2000).

[10] T. Sasamoto and H. Spohn, One-dimensional Kardar-Parisi-Zhang equation: An exact solution and its universality, Phys. Rev. Lett. **104**, 230602 (2010).

[11] Herbert Spohn, Exact solutions for KPZ-type growth processes, random matrices, and equilibrium shapes of crystals, Physica A **369**, 71 (2006).

[12] Gideon Amir, Ivan Corwin, and Jeremy Quastel, Probability distribution of the free energy of the continuum directed random polymer in $1+1$ dimensions, Commun. Pure Appl. Math. **64**, 466 (2011).

[13] V. Dotsenko, Bethe ansatz derivation of the Tracy-Widom distribution for one-dimensional directed polymers, Europhys. Lett. **90**, 20003 (2010).

[14] Victor Dotsenko and Boris Klumov, Bethe ansatz solution for one-dimensional directed polymers in random media, J. Stat. Mech.: Theory Exp. (2010) P03022.

[15] Pasquale Calabrese, Pierre Le Doussal, and Alberto Rosso, Free-energy distribution of the directed polymer at high temperature, Europhys. Lett. **90**, 20002 (2010).

[16] Pierre Le Doussal and Pasquale Calabrese, The KPZ equation with flat initial condition and the directed polymer with one free end, J. Stat. Mech.: Theory Exp. (2012) P06001.
[17] Mehran Kardar and Yi-Cheng Zhang, Scaling of directed polymers in random media, Phys. Rev. Lett. **58**, 2087 (1987).
[18] D. A. Huse, C. L. Henley, and D. S. Fisher, Huse, Henley, and Fisher respond, Phys. Rev. Lett. **55**, 2924 (1985).
[19] Francesca Colaiori and M. A. Moore, Upper critical dimension, dynamic exponent, and scaling functions in the mode-coupling theory for the Kardar-Parisi-Zhang equation, Phys. Rev. Lett. **86**, 3946 (2001).
[20] Timothy Halpin-Healy, (2+1)-dimensional directed polymer in a random medium: Scaling phenomena and universal distributions, Phys. Rev. Lett. **109**, 170602 (2012).
[21] Timothy Halpin-Healy, Extremal paths, the stochastic heat equation, and the three-dimensional Kardar-Parisi-Zhang universality class, Phys. Rev. E **88**, 042118 (2013).
[22] Jeffrey Kelling and Géza Ódor, Extremely large-scale simulation of a Kardar-Parisi-Zhang model using graphics cards, Phys. Rev. E **84**, 061150 (2011).
[23] Vladimir G. Miranda and Fábio D. A. Aarão Reis, Numerical study of the Kardar-Parisi-Zhang equation, Phys. Rev. E **77**, 031134 (2008).
[24] Thomas Kloss, Léonie Canet, and Nicolás Wschebor, Nonperturbative renormalization group for the stationary Kardar-Parisi-Zhang equation: Scaling functions and amplitude ratios in $1+1$, $2+1$, and $3+1$ dimensions, Phys. Rev. E **86**, 051124 (2012).
[25] Moshe Schwartz and Ehud Perlsman, Upper critical dimension of the Kardar-Parisi-Zhang equation, Phys. Rev. E **85**, 050103 (2012).
[26] Yi-Cheng Zhang, Growth anomaly and its implications, Physica A **170**, 1 (1990).
[27] Joachim Krug, Kinetic roughening by exceptional fluctuations, J. Phys. I **1**, 9 (1991).
[28] Giulio Biroli, Jean-Philippe Bouchaud, and Marc Potters, Extreme value problems in random matrix theory and other disordered systems, J. Stat. Mech.: Theory Exp. (2007) P07019.
[29] Bernard Derrida and Herbert Spohn, Polymers on disordered trees, spin glasses, and traveling waves, J. Stat. Phys. **51**, 817 (1988).
[30] Kurt Johansson, Transversal fluctuations for increasing subsequences on the plane, Probab. Theory Relat. Fields **116**, 445 (2000).
[31] Michael Praehofer and Herbert Spohn, Universal distributions for growth processes in $1+1$ dimensions and random matrices, Phys. Rev. Lett. **84**, 4882 (2000).
[32] Timo Seppalainen, Scaling for a one-dimensional directed polymer with boundary conditions, Ann. Probab. **40**, 19 (2012).
[33] Ivan Corwin, Neil O'Connell, Timo Seppalainen, and Nikolaos Zygouras, Tropical combinatorics and Whittaker functions, Duke Math. J. **163**, 513 (2014).
[34] Alexei Borodin, Ivan Corwin, and Daniel Remenik, Log-gamma polymer free energy fluctuations via a Fredholm determinant identity, Commun. Math. Phys. **324**, 215 (2013).
[35] Thimothée Thiery and Pierre Le Doussal, Log-gamma directed polymer with fixed endpoints via the replica Bethe ansatz, J. Stat. Mech. (2014) P10018.
[36] Ulrich Schulz, Jean Villain, Edouard Brézin, and Henri Orland, Thermal fluctuations in some random field models, J. Stat. Phys. **51**, 1 (1988).
[37] Ben Hambly and James B. Martin, Heavy tails in last-passage percolation, Probab. Theory Relat. Fields **137**, 227 (2007).
[38] Chi-Hang Lam and Leonard M. Sander, Surface growth with power-law noise, Phys. Rev. Lett. **69**, 3338 (1992).
[39] Kazumasa A. Takeuchi and Masaki Sano, Universal fluctuations of growing interfaces: Evidence in turbulent liquid crystals, Phys. Rev. Lett. **104**, 230601 (2010).
[40] Thomas Gueudré and Pierre Le Doussal, Statistics of shocks in a toy model with heavy tails, Phys. Rev. E **89**, 042111 (2014).
[41] Patrik L. Ferrari, From interacting particle systems to random matrices, J. Stat. Mech.: Theory Exp. (2010) P10016.
[42] Kurt Johansson, Discrete polynuclear growth and determinantal processes, Commun. Math. Phys. **242**, 277 (2003).
[43] Michael Praehofer and Herbert Spohn, Scale invariance of the PNG droplet and the Airy process, J. Stat. Phys. **108**, 1071 (2002).
[44] Alexei Borodin, Patrik L. Ferrari, Michael Praehofer, and Tomohiro Sasamoto, Fluctuation properties of the TASEP with periodic initial configuration, J. Stat. Phys. **129**, 1055 (2007).
[45] Jeremy Quastel and Daniel Remenik, Local behavior and hitting probabilities of the Airy_1 process, Probab. Theory Relat. Fields **157**, 605 (2013).
[46] Jeremy Quastel and Daniel Remenik, Airy processes and variational problems, in *Topics in Percolative and Disordered Systems*, edited by Alejandro F. Ramirez, Gerard Ben Arous, Pablo A. Ferrari, Charles M. Newman, Vladas Sidoravicius, and Maria Eullia Vares, Springer Proceedings in Mathematics and Statistics Vol. 69 (Springer, New York, 2014), pp. 121–171.
[47] Antonio Auffinger and Oren Louidor, Directed polymers in a random environment with heavy tails, Commun. Pure Appl. Math. **64**, 183 (2010).
[48] Gregory Schehr, Extremes of n vicious walkers for large n: Application to the directed polymer and KPZ interfaces, J. Stat. Phys. **149**, 385 (2012).
[49] Gregorio Moreno Flores, Jeremy Quastel, and Daniel Remenik, Endpoint distribution of directed polymers in $1+1$ dimensions, Commun. Math. Phys. **317**, 363 (2013).
[50] Jinho Baik, Karl Liechty, and Grégory Schehr, On the joint distribution of the maximum and its position of the Airy_2 process minus a parabola, J. Math. Phys. **53**, 083303 (2012).
[51] Pierre Le Doussal, Exact results and open questions in first principle functional RG, Ann. Phys. (NY) **325**, 49 (2010).
[52] Pierre Le Doussal, Kay Jörg Wiese, and Pascal Chauve, Functional renormalization group and the field theory of disordered elastic systems, Phys. Rev. E **69**, 026112 (2004).
[53] Harry Kesten, Random difference equations and renewal theory for products of random matrices, Acta Math. **131**, 207 (1973).